

COPPER ADSORPTION ONTO POMEGRANATE PEEL ACTIVATED CARBON AS A NEW ADSORBENT

Wafa Saadi, Souad Souissi-Najar, Mariem Othman and
Abdelmottaleb Ouederni

National School of Engineers of Gabes, University of Gabes, 6029 Gabes, Tunisia

✉ *Corresponding author: W. Saadi, saadiwafa@yahoo.fr*

Received September 22, 2022

Pomegranate peel-based activated carbon was prepared using phosphoric acid impregnation for removing copper ions from aqueous solutions. The activated carbon sample was characterized using N₂ adsorption–desorption isotherms, SEM, FTIR, and Boehm titration. Batch adsorption experiments were performed as a function of initial pH, contact time, initial ion concentration and temperature. The metal adsorption was found pH dependent, with maximum adsorption occurring at an initial pH of 5.4. Langmuir, Freundlich and Temkin isotherms were used to analyze the equilibrium data at different temperatures. The Freundlich isotherm was considered to be the best model for representing Cu(II) adsorption data. The kinetic studies were analyzed using pseudo-first order, pseudo-second order and intraparticle diffusion models, with good fitting to the pseudo-second-order model. The adsorption behavior of the binary solution system Cu(II)-Cd(II) showed that the adsorbent has higher selectivity towards copper ions than cadmium ions.

Keywords: activated carbon, adsorption, heavy metal, pomegranate peels

INTRODUCTION

Metallic elements always exist in different forms in the environment as a result of natural causes or certain human activities. In trace amounts, they are necessary for living beings.¹ However, in high concentrations, they exhibit high- or low-level toxicity.² This may pose particular problems because they accumulate and are not biodegradable in the environment.³ The heavy metals associated with the concept of pollution and toxicity, are generally arsenic (As), cadmium (Cd), chromium (Cr), copper (Cu), mercury (Hg), manganese (Mn), nickel (Ni), lead (Pb), tin (Sn) and zinc (Zn).

Various techniques, such as precipitation, flocculation, ion exchange, electrolysis and membrane processes, can be used to remove heavy metals from aqueous solutions. However, these methods are expensive and can lead to the formation of other intermediate dangerous compounds. Thus, the selection of inexpensive alternative technologies to treat these pollutants is very important. Adsorption has the advantage to

be applied in the treatment of various effluents, providing an answer to regulatory requirements for environmental protection. Several adsorbents have been investigated for wastewater treatment, including zeolite, silica gel and activated carbon.⁴ Previous research studies have shown that activated carbon can be a good adsorbent.⁵⁻⁸

Activated carbons prepared from various agricultural wastes have been used as adsorbents to remove copper ions from aqueous solutions.^{5,7-13} Only El-Ashtoukhy *et al.*¹⁴ investigated the copper adsorption capacity of activated carbon based on pomegranate peels before, while a few other studies have also been reported on the use of pomegranate peels as a new adsorbent developed for environmental protection.¹⁵⁻¹⁸ Pomegranate peels are a by-product of the pomegranate juice industry. Their abundance and ability to retain pollutants make them good adsorbents.¹⁹⁻²³ In recently published research,^{19,22,24} pomegranate peels are used to prepare chemically activated carbons using KOH, H₃PO₄ and H₃PO₄-steam as

activating agents. The resulting activated carbons have very interesting texture and adsorption characteristics. This encouraging result, as well as the wide availability of this agricultural waste in the southern region of Tunisia, has motivated us to use pomegranate peels for preparing an activated carbon adsorbent for the purpose of water treatment.

In this work, pomegranate peel activated carbon was evaluated for the removal of copper ions from aqueous solutions. The effects of pH solution, contact time, initial copper concentration and temperature in the adsorption process were examined. FTIR analysis was carried out to understand the surface functional groups of the adsorbent. Equilibrium data were analyzed by different equilibrium isotherm models. Kinetic data were evaluated by the pseudo-first order and pseudo-second order models. Thermodynamic parameters, such as free energy (ΔG), enthalpy (ΔH) and entropy (ΔS), were also determined to understand the spontaneity and the type of the adsorption process.

EXPERIMENTAL

Chemicals

Copper nitrate (99.5%) utilized in the present study was of analytical grade. A heavy metal stock solution of 100 mg/L was prepared by dissolving required amounts of $\text{Cu}(\text{NO}_3)_2$ in double-distilled water. Lower metal concentrations were obtained by simple dilution.

Preparation of activated carbon

The pomegranate peel activated carbon "PPAC" was obtained by chemical activation, on the basis of previous work.²² Briefly, the pomegranate peels were impregnated with H_3PO_4 solution for 2 hours under boiling conditions ($\approx 112^\circ\text{C}$). The samples were then activated under nitrogen flow, at a heating rate of $10^\circ\text{C}/\text{min}$ up to 400°C during 2 hours. The obtained products were washed several times with hot distilled water and dried at 110°C overnight and then sieved to the desired particle sizes to be used for adsorption experiments.

Characterization of activated carbon

The adsorption isotherm of nitrogen onto the AC was determined at 77 K, using a Micrometrics ASAP 2420 volumetric adsorption system. The specific surface area (S_{BET}) was calculated based on the Brauner-Emmet-Teller (BET) theory.

Total pore volume was estimated from N_2 adsorption at a relative pressure of 0.99. Total micropore volume (VDR_{N_2}) was assessed by the Dubinin-Radushkevich (DR) equation, applying to the

appropriate adsorption data. The mesopore adsorption volume (V_{meso}) was calculated by the BJH (Barrett-Joyner-Halenda) model. These calculations were performed by the apparatus software.

Surface chemistry was characterized by Boehm titration and the pH at the point of zero charge (pH_{PZC}) was determined according to the experimental procedure described elsewhere.²²

For studying the vibrational modes of the PPAC functional groups, its FTIR spectrum was measured in the 4000 and 400 cm^{-1} range, using a Spectrum Two Perkin Elmer Spectrometer equipped with a DTGS detector, with a resolution of 2 cm^{-1} and 32 scans.

Batch equilibrium adsorption

The effect of initial pH was studied by performing adsorption experiments, which were carried out as follows: 0.1 g of activated carbon was mixed with a 50 mL of copper solution of 40 mg/L. The pH was adjusted from 2 to 10, by using 0.1 N HCl or 0.1 N NaOH solutions. After adsorption, the pH value that allowed maximum copper removal was measured.

To study the effect of initial copper concentration, adsorption experiments were carried out by introducing a 0.1 g of PPAC into a series of Erlenmeyer flasks containing 50 mL of metal solution, with different initial concentration. The mixture was shaken for 140 min at pH 5.4. The adsorption of copper from aqueous solutions was also carried out at different temperatures (30, 40, 50 and 60°C).

To study the copper adsorption kinetics, a volume of 1 L of metal ion solution with each initial concentration of 20, 40, and 70 mg/L was poured into a jacketed reactor maintained at a fixed stirring speed of 200 rpm. When the desired value (30°C) of solution temperature was reached, 2 g of the PPAC were added.

Particle size was also considered an important parameter affecting the adsorption kinetics, as it governs the diffusion of the adsorbate into the adsorbent particles. The adsorption kinetic experiments were performed using various average diameter of PPAC particles (<0.2 mm, 0.2-0.6 mm, 0.6-0.8 mm). All experiments were carried out under the same conditions, with a copper initial concentration of 50 mg/L.

Experiments of binary adsorption isotherms, using both copper and cadmium ions, were performed under the same conditions as for single metal adsorption isotherms. Initial copper concentration was varied from 10 to 90 mg/L, while the initial cadmium concentration was fixed at 40 mg/L. The adsorption tests were carried out discontinuously, in a series of Erlenmeyer flasks, into which a volume of 50 mL of an aqueous solution of copper-cadmium was introduced, and then 0.1 g of activated carbon was added.

The heavy metal ion concentrations of the samples filtrated through a $0.45\text{-}\mu\text{m}$ syringe filter were analyzed using an inductively coupled plasma atomic

emission spectrometer (ICP-AES; Activa-M, HORIBA Jobin Yvon).

The amount of metal ion adsorbed by PPAC was calculated using the following equation:

$$q_{ads} = \frac{(C_0 - C_f)V}{m_{CA}} \quad (1)$$

where q_{ads} is the metal ion uptake (mg/g), C_0 – copper initial concentration, C_f – copper final concentration, m – the weight of PPAC (g) and V is the volume of solution in the flask (L).

Modeling of adsorption isotherms

The three most commonly used adsorption equilibrium models are the Langmuir, Freundlich and Temkin ones.

Langmuir's theory is very useful for the monomolecular adsorption of a solute that forms a monolayer on the surface of an adsorbent.²⁵ It is described by the following expression:

$$q_e = \frac{q_{max}K_L C_e}{1 + K_L C_e} \quad (2)$$

where C_e – concentration at equilibrium (mg/L), q_e – quantity of product adsorbed per unit mass of adsorbent (mg/g), q_{max} – maximum theoretical adsorption capacity (mg/g), K_L – constant of thermodynamic adsorption equilibrium (L/mg).

The Freundlich model is based on the distribution of pollutants between the surface of the adsorbent and the fluid phase at equilibrium.²⁶ The Freundlich equation is as follows:

$$q_e = K_f C_e^{n_f} \quad (3)$$

where K_f is an indication of the adsorption capacity of the adsorbent, n_f represents the intensity of adsorption and indicates whether the adsorption is favorable. If $n_f = 1$, the adsorption is linear, if $n_f < 1$, the adsorption is chemical, and if $n_f > 1$, the adsorption is physical and favorable.

The Temkin model describes the effects of indirect adsorbent–adsorbate interaction on adsorption isotherms, suggesting that, due to these interactions, the heat of adsorption of all molecules on the same layer decreases linearly with the rate of surface coverage.²⁷

The model is given by the following equation:

$$q_e = \frac{RT}{b} \ln(A) + \frac{RT}{b} \ln(C_e) \quad (4)$$

where R – ideal gas constant ($R = 8.314 \text{ J}\cdot\text{mol}^{-1}\cdot\text{K}^{-1}$), T – temperature (K), A – model constant (L/g).

Kinetic modeling

Pseudo-first order model

The pseudo-first order model or Lagergren model²⁸ is expressed in the following differential form:

$$\frac{dq_t}{dt} = k_1 (q_e - q_t) \quad (5)$$

where k_1 is the rate constant of the pseudo-first order model (min^{-1}), q_e is the adsorption capacity at equilibrium ($\text{mol}\cdot\text{g}^{-1}$), q_t is the adsorption capacity at time t ($\text{mol}\cdot\text{g}^{-1}$) and t is the time (min). By integrating Equation (5) between the initial and final time, the following relation is obtained:

$$q_t = q_e (1 - e^{-k_1 t}) \quad (6)$$

The linearization of the previous equation gives:

$$\ln(q_e - q_t) = \ln q_e - k_1 t \quad (7)$$

The kinetic parameters of this model can be obtained by plotting the line $\ln(q_e - q_t) = f(t)$.

Pseudo-second-order model (PSO)

The pseudo-second-order model was proposed by Ho and McKay.²⁹ It makes it possible to characterize the adsorption kinetics by taking into account both the case of rapid binding of solutes on the most reactive sites and that of slow binding at sites of low energy, its expression is given by Equation (8):

$$\frac{dq_t}{dt} = k_2 (q_e - q_t)^2 \quad (8)$$

where k_2 – is the second order adsorption reaction rate constant ($\text{g}\cdot\text{mg}^{-1}\cdot\text{min}^{-1}$), q_e – is the amount adsorbed at equilibrium (mg/g), q_t – is the amount adsorbed at time t (mg/g), t – contact time (min).

After integration, we get Equation (9):

$$q_t = \frac{k_2 q_e^2 t}{k_2 q_e t + 1} \quad (9)$$

The linearization of the previous equation gives:

$$\frac{t}{q_t} = \frac{1}{k_2 q_e^2} + \frac{1}{q_e} t \quad (10)$$

A straight line is obtained by plotting t/q_t as a function of contact time. Then, the slope and the y-intercept give the values of q_e and the kinetic constant k_2 .

Intraparticle diffusion model

The intraparticle diffusion model is represented by the following equation:

$$q_t = k_{int} \sqrt{t} + C \quad (11)$$

where q_t is the amount adsorbed at time t (mg/g), C – the intersection of the line with the ordinate axis. The value of C gives an idea of the thickness of the boundary layer, because the greater the value the larger the intercept, the greater the effect of the boundary layer. Also, k_{int} is the intraparticle diffusion constant ($\text{mg}/\text{g}\cdot\text{min}^{1/2}$).

Gibbs free energy

In order to confirm the nature of the adsorption process, the important thermodynamic parameters, such as the standard Gibbs free energy, ΔG° , enthalpy, ΔH° , and entropy, ΔS° , can be estimated from the following equations:³⁰

$$\Delta G^\circ = -RT \ln(1000K_d) \quad (12)$$

$$\ln(1,000K_d) = \frac{-\Delta H^\circ}{R} \times \frac{1}{T} + \frac{\Delta S^\circ}{R} \quad (13)$$

The distribution coefficient (K_d) was defined in Equation (14):

$$K_d = \frac{q_e}{c_e} \quad (14)$$

where R is the universal gas constant (8.314 J/mol. K), and T is the absolute temperature (K).

RESULTS AND DISCUSSION

Physico-chemical characteristics

Surface oxygen-containing functional groups

The FTIR spectrum of PPAC is illustrated in Figure 1. It has been reported that some decomposition of functional groups in the form of volatile matter occurs in the activation process at high temperature.³¹ The broad and intense absorption peaks in the 3700–3100 cm^{-1} correspond to the O-H stretching vibrations of cellulose, pectin, absorbed water, hemicelluloses and lignin.³² The band at 3690 cm^{-1} corresponds to hydroxyl OH functional groups, probably due to adsorbed water. The peak at 2990 cm^{-1} is attributed to asymmetric

and symmetric aliphatic methyl group in PPAC.³³ The band at 2340 cm^{-1} corresponds to the stretching of alkynes group.³⁴ Two other small peaks can be observed. The stretching peaks from 1210 to 1570 cm^{-1} correspond to the presence of C–O (carboxyl) and C=O (carbonyl) groups, which shows the presence of carbonyl carboxylates on the surface of PPAC.³⁴ When pomegranate peels are activated with phosphoric acid, the bands that appear between 900 and 1200 cm^{-1} may be attributed to the presence of phosphorus species in the sample.

Other surface functional groups

The surface functional groups of the pomegranate peel activated carbon, determined by the Boehm method, are shown in Figure 2. The PPAC has an acidic character, as illustrated by the high acid equivalent amount, which is equal to 1.4 meq/g. This result is in agreement with the values of pH_{pzc} measured as described below.

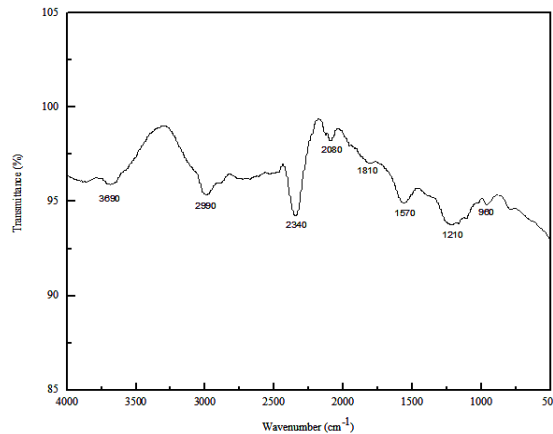


Figure 1: Infrared spectrum of PPAC

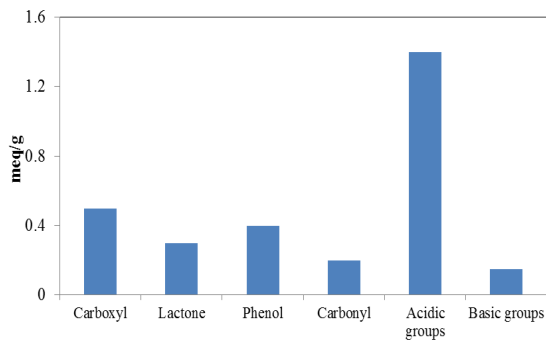


Figure 2: Relative contents of surface functional groups of PPAC

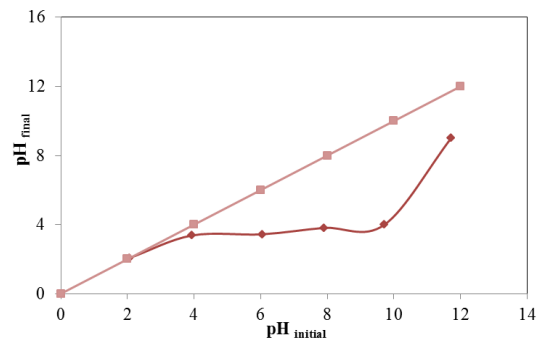


Figure 3: Isoelectric pH of PPAC

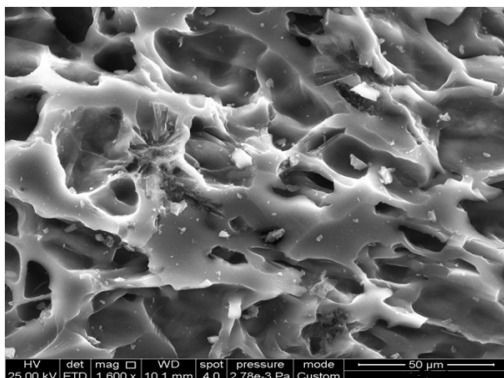


Figure 4: SEM image of PPAC

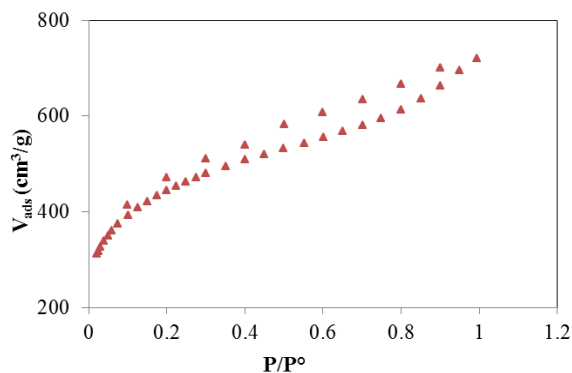
Figure 5: N₂ adsorption-desorption isotherm of PPAC at 77 K

Table 1
Porosity of activated carbon based on pomegranate peels

	S_{BET} (m ² /g)	V_{tot} (cm ³ /g)	V_{mic} (cm ³ /g)	V_{mes} (cm ³ /g)	D_p (nm)	Iodine number
PPAC	1597	1.118	1.002	0.116	2.99	813

The pH of suspension and pH_{pzc}

The suspension pH of the prepared activated carbon is 3.12, which gives it an acidic character. This acidity is related to the type of activation that involves the use of phosphoric acid as an activating agent. Plotting the curve $\text{pH}_{\text{final}} = f(\text{pH}_{\text{initial}})$, as well as the first bisector $\text{pH}_{\text{final}} = \text{pH}_{\text{initial}}$, allows us to deduce the pH value at the point of zero charge of PPAC (Fig. 3), which corresponds to the intersection of the two curves.

The acid-base surface properties of PPAC are very important, and even seem to prevail over its porosity characteristics in the case of organic compounds adsorption from the aqueous phase. From Figure 3, it can be seen that the pH_{pzc} value is 2.8. Therefore, the adsorption of cations will be favorable for pH values higher than pH_{pzc} (negatively charged surface).

Scanning electron microscopy (SEM)

The SEM image in Figure 4 shows that the external surface of the PPAC is full of cavities. It seems that the cavities on the surfaces of carbons resulted from the evaporation of the phosphoric acid, representing the space previously occupied by the activating agent.³⁵ The impregnation with H₃PO₄, followed by a thermal treatment under inert atmosphere, involves a remarkable degradation of the microstructure.³⁵

Textural characterization of the adsorbent

The adsorption-desorption isotherms of nitrogen at 77 K obtained on PPAC are shown in Figure 5. The adsorption isotherm is type IV according to the IUPAC classification.³⁶ The adsorption isotherm shows a sharp increase in adsorbed volume up to P/P° of 0.1, which was attributed to the presence of micropores. However, a gradual increase in this volume throughout the relative pressure range could be attributed to the presence of mesopores. Furthermore, the presence of a small hysteresis loop in the adsorption-desorption isotherms confirms the existence of this mesoporosity.²²

The total pore volume of PPAC is 1.118 cm³/g, while the volume of mesopores represents 0.116 cm³/g. The main textural characteristics of PPAC are presented in Table 1.

Adsorption study

Effect of contact time

Determining the contact time to reach adsorption equilibrium is an important step in the study of adsorption kinetics. The effect of contact time on copper adsorption is given in Figure 6. The plotted curve shows that equilibrium is reached quickly. Adsorption is very rapid at the start of contact between the adsorbate and the adsorbent, due to the existence of a large number of free sites, which explains the significant slope of the curves after the first minutes of contact. A

two-step adsorption mechanism is widely reported in the literature, in which the first adsorption mechanism is fast and quantitatively dominant, and the second adsorption mechanism is slow and quantitatively negligible.³⁷

The activated carbon shows good performance during the first 30 minutes of copper adsorption, and then stabilizes to reach equilibrium. This means that the mass transfer resistance of copper on the adsorption surface is low. The adsorption equilibrium was relatively fast and was reached in about 140 min. This equilibrium time is very short, compared with other literature results,^{5,38-43} which is one of the advantages of the prepared PPAC.

Effect of initial pH

The effect of initial solution pH is shown in Figure 7. It is clear that the PPAC adsorption capacity increased from 3.509 to 7.037 mg/g as the pH increased from 2 to 6. Above pH 6, copper precipitation reduces the adsorption capacity. Therefore, copper adsorption conditions must be

considered at a pH below this value. In this pH range, the copper is in the Cu²⁺ form.

According to Rao *et al.*,⁹ the effect of pH is directly related to the surface charge of the adsorbent material, which is positive for a pH lower than the isoelectric pH and, in this case, the metal is weakly adsorbed due to electrostatic repulsions. Increasing the pH beyond the isoelectric pH makes the surface charge more negative and hence the amount adsorbed increases. Based on these results, further kinetic and equilibrium experiments will be carried out at an optimum initial pH of 5.4.

Effect of temperature

Temperature is an important factor governing the adsorption process. The effect of this parameter on the copper adsorption onto PPAC was studied at four temperatures: 30, 40, 50 and 60 °C. The metal ion concentration varied between 10 mg/L and 90 mg/L and the activated carbon dose was 0.1 g/L.

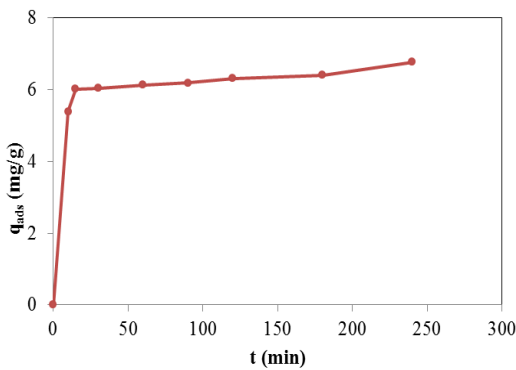


Figure 6: Effect of contact time on copper adsorption onto PPAC at T = 30 °C

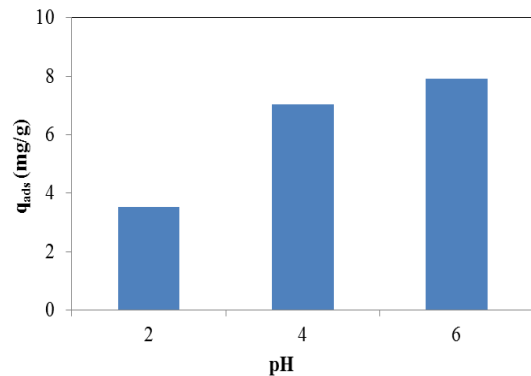


Figure 7: Copper ions uptake by PPAC as a function of initial solution pH (C₀ = 40 mg/L, equilibrium time = 140 min, T = 30 °C)

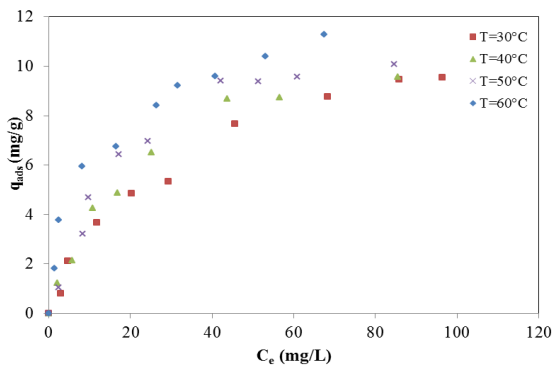


Figure 8: Effect of temperature on copper ion adsorption onto PPAC

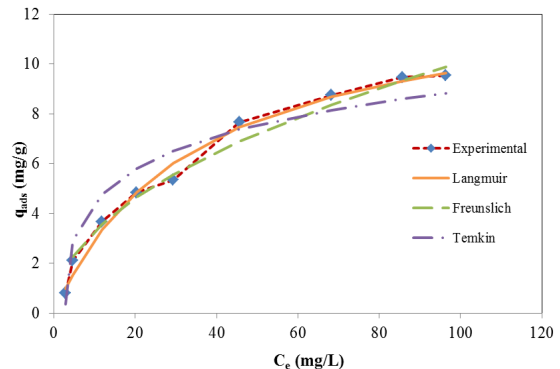


Figure 9: Modeling of adsorption isotherm (m = 0.1 g, 0.2 mm < dp < 0.6 mm, T = 30 °C, pH 5.4)

Table 2
Isotherm model parameters for copper adsorption onto PPAC

Model	Parameters	T = 30 °C	T = 40 °C	T = 50 °C	T = 60 °C
Langmuir	q_{exp} (mg/g)	9.54	9.57	10.06	11.27
	q_{max} (mg/g)	9.62	9.56	10.41	10.45
	K_L (L/g)	0.02	0.04	0.05	0.12
	R^2	0.98	0.98	0.98	0.95
Freundlich	K_f	1.08	1.34	1.98	2.55
	n_f	2.07	2.17	2.59	2.79
	R^2	0.98	0.99	0.99	0.99
Temkin	A (L/g)	0.14	0.28	0.21	3.46
	B (J/mol)	1.93	2.05	2.27	2.63
	R^2	0.92	0.98	0.93	0.96

As illustrated in Figure 8, the amount of copper adsorbed increases with increasing temperature from 30 to 60 °C. It can, therefore, be concluded that the adsorption is endothermic. Likewise, Shou *et al.*⁴⁴ and Weng *et al.*⁴⁵ found that the adsorption rate of copper ions increased with increasing solution temperatures from 20 to 40 °C, and from 5 to 50 °C, respectively.

The enhancement in the adsorption capacity might be due to the chemical interaction between the adsorbate and the adsorbent, the creation of some new adsorption sites, or the increased rate of intraparticle diffusion of adsorbate molecules into the pores of the activated carbons at higher temperature. The process is, therefore, favored at high temperature. Similar findings have been reported by other researchers working on the removal of heavy metal ions from aqueous solution by activated carbon.⁴⁶⁻⁴⁷

To describe the phenomenon of copper adsorption on PPAC, different equilibrium models have been applied, namely the models of Langmuir, Freundlich and Temkin. The fitting of the experimental results to the models is presented in Figure 9. As Table 2 depicts, copper adsorption onto PPAC has a high compliance with the Freundlich model ($R^2 = 0.99$). This shows that the surface of the adsorbent is heterogeneous and the adsorption of copper on the adsorbent occurs in multilayer. This finding is in line with the results reported previously by El-Ashtoukhy *et al.*¹⁴ and Rao and Rehman.⁴⁸ Furthermore, the values of the n coefficient in the Freundlich model indicate the high tendency toward adsorbing the copper onto the PPAC.

Kinetic study

Kinetic studies of heavy metal adsorption are of great importance, as they allow determining the

factors involved in the adsorption process. The effect of some parameters on the copper adsorption kinetics was investigated, such as the initial concentration of metal ions and the size of the activated carbon particles.

Influence of adsorption time and initial concentration of adsorbate

The effect of the initial metal concentration on the adsorption capacity of PPAC was studied for concentration values of 20, 40 and 70 mg/L at pH equal to 5.8, as shown in Figure 10. It is apparent that the adsorbed amounts of Cu(II) increased from 3.204 mg/g to 9.204 mg/g due to the high quantity of copper ions in the concentrated solution.⁴⁹

Effect of adsorbent particle size

The results shown in Figure 11 indicate that the adsorbed amount of copper increases over time until it reaches a constant value. It is clear that the decrease in particle size led to an increase in the adsorbed capacity of copper. Adsorption is a surface phenomenon; therefore a smaller particle size provides a relatively larger and more accessible surface area and therefore greater adsorption equilibrium.⁵⁰

Application of kinetic models

It is important to find the rate-limiting step of the adsorption process. For this reason, we tested kinetic models that are commonly applied to suspensions, namely, the pseudo-first order model, the pseudo-second order model and the intraparticle diffusion model.

Pseudo-first and -second order models

The experimental results were first fitted to the pseudo-first order model. Figure 12 (a and b)

gives the plotting of $\ln(q_e - q_t)$ as a function of time. This representation makes it possible to deduce the adsorption capacities and the values of the R^2 regression coefficients for various concentrations and various particle sizes.

The linear form of the pseudo-second order model is obtained by plotting t/q_t as a function of time. Figure 13 (a and b) illustrates the modeling of the copper adsorption kinetic data to the pseudo-second order model. The curves obtained are straight lines with regression coefficients close to unity and maximum predicted adsorbed

quantities close to the experimental ones. This shows the validity of this model.

Based on the results in Table 3, it can be noted that the pseudo-second order model is the most reliable for determining the copper ion adsorption kinetics, as it presents the best fit to the data ($R^2 = 0.99$). Indeed, the equilibrium adsorption capacity values calculated by this model are very close to the experimentally determined values. Therefore, we can assume that the pseudo-second order model is the one that describes best the copper adsorption process using PPAC as a new adsorbent.

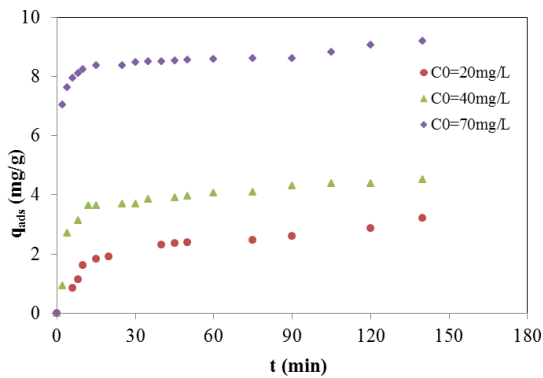


Figure 10: Experimental results of Cu (II) adsorption on PPAC in terms of initial concentration (T 30 °C; pH 5.4)

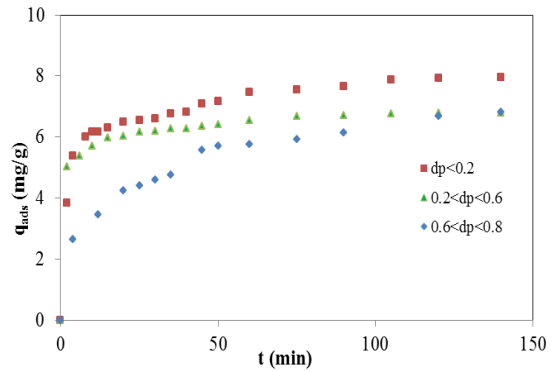


Figure 11: Effect of adsorbent particle size onto adsorption capacity

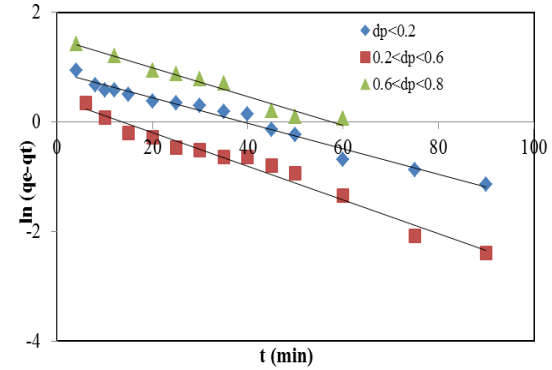
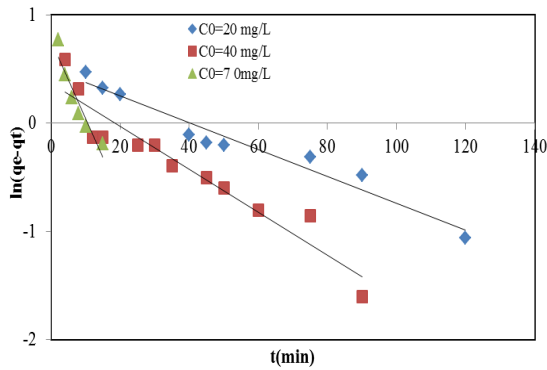


Figure 12: Pseudo-first order model for different initial concentrations of Cu (II) (a) and adsorbent particle sizes (b)

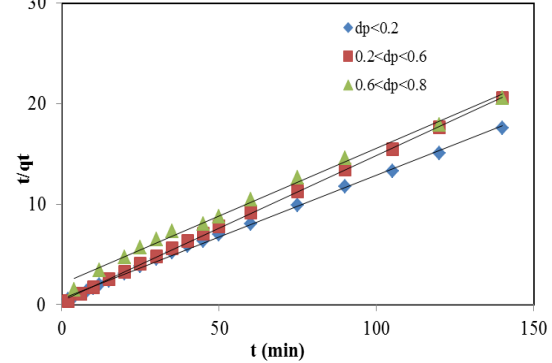
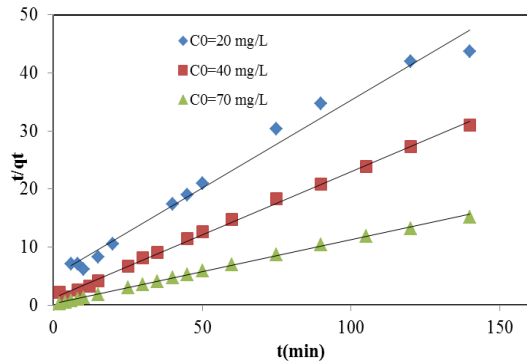


Figure 13: Pseudo-second order model for different initial concentrations of Cu (II) (a) and adsorbent particle sizes (b)

Table 3
Kinetic parameters of pseudo-first and pseudo-second order models of Cu(II) adsorption onto PPAC

C ₀ (mg/L)	Pseudo-first order				Pseudo-second order			
	k ₁ (min ⁻¹)	R ²	q _{exp} (mg/g)	q _{model} (mg/g)	k ₂ (g.mg ⁻¹ min ⁻¹)	R ²	q _{model} (mg/g)	
20	0.01	0.95	3.20	1.64	0.01	0.98	3.3	
40	0.02	0.93	4.51	1.42	0.03	0.99	4.6	
70	0.01	0.87	9.20	1.07	0.05	0.99	9.09	
dp (mm)	k ₁ (min ⁻¹)	R ²	q _{exp} (mg/g)	q _{model} (mg/g)	k ₂ (g.mg ⁻¹ min ⁻¹)	R ²	q _{model} (mg/g)	
dp < 0.2	0.02	0.97	7.97	2.48	0.02	0.99	8.19	
0.2 < dp < 0.6	0.03	0.97	6.79	1.53	0.05	0.99	6.94	
0.6 < dp < 0.8	0.02	0.96	6.81	4.58	0.008	0.99	7.4	

Intraparticle diffusion model

In order to better understand the process of heavy metal adsorption, the model of intraparticle diffusion was studied for different initial concentrations and different particle sizes. Figure 14 (a and b) presents the intraparticle diffusion model by plotting q_t as a function of t^{0.5}.

The curves representing q_t as a function of t^{0.5} are linear and have three parts, which shows the presence of three stages governing the adsorption onto PPAC. The first stage is assigned

to external mass transfer. Indeed, the presence of a large number of active sites on the surface of activated carbon leads to an increase in adsorption kinetics during the first step.⁵¹ In the second step, the possibility of blocking the pores and the steric hindrance exerted by the molecules adsorbed on the surface of the adsorbent makes it possible to slow down the adsorption process.⁵ During the last step, the adsorption reaches equilibrium. All copper initial concentration lines did not pass through the origin.

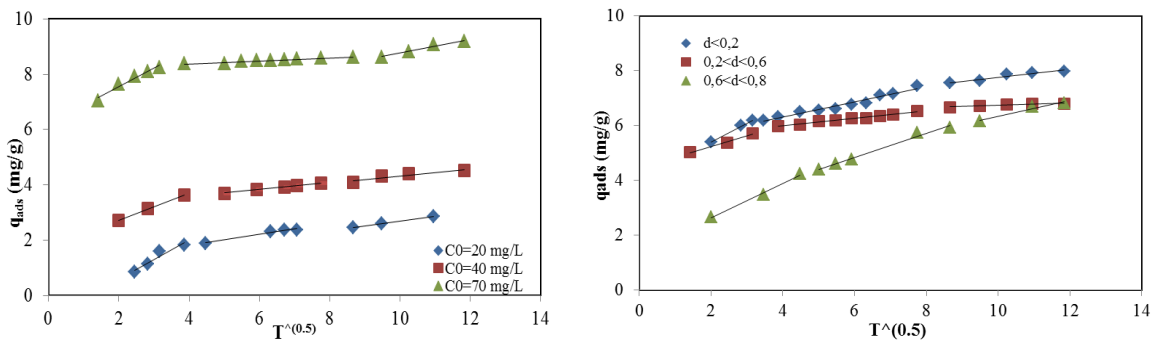


Figure 14: Modeling of intraparticle diffusion for different initial Cu (II) concentrations (a) and different adsorbent particle sizes (b)

Table 4
Parameters of intraparticle diffusion model

Parameters	C ₀ (mg/L)			dp (mm)		
	20	40	70	0.6 < d _p < 0.8	0.2 < d _p < 0.6	d _p < 0.2
K ₁ (mg/g.min ^{1/2})	0.697	0.490	0.673	0.63	0.385	0.683
C	-0.795	1.744	6.196	1.367	4.470	4.037
R ²	0.908	0.999	0.958	0.991	0.993	0.996
K ₂ (mg/g.min ^{1/2})	0.198	0.129	0.055	0.439	0.137	0.279
C	1.023	3.058	8.149	2.211	5.442	5.185
R ²	0.984	0.991	0.940	0.984	0.977	0.961
K ₃ (mg/g.min ^{1/2})	0.169	0.125	0.253	0.290	0.043	0.143
C	0.995	3.068	6.230	3.428	6.308	9.326
R ²	0.995	0.893	0.978	0.959	0.879	0.907

Table 5
Thermodynamic parameters for the adsorption of Cu(II) onto PPAC

T (K)	ΔG° (kJ.mol ⁻¹)	ΔH° (kJ.mol ⁻¹)	ΔS° (J.mol ⁻¹ K ⁻¹)
303.15	-13.801		
313.15	-14.788		
323.15	-15.775	15.813	97.689
333.15	-16.732		

This indicates that the adsorption of copper on the prepared activated carbon is mainly governed by external mass transport, where particle diffusion was the rate-limiting step.⁵²

The parameters of the intraparticle diffusion model are given in Table 4. Examining these parameters, it may be noted that all parts are well fitted by the intraparticle diffusion equation, with high correlation coefficients.

Table 5 shows that the rate constants K_1 , of the first part, is higher than the K_2 and K_3 values of the two other parts, because the first adsorption stage was faster than the diffusion in the pores of PPAC, as shown in Figure 14 (a and b).

Thermodynamic study

The thermodynamic parameters obtained are summarized in Table 5. The data indicate that the adsorption of copper ions onto PPAC is a physical process, which is defined by the ΔH° value (15.813 kJ.mol⁻¹) between 2.1 and 20.9 kJ.mol⁻¹.⁵³ The endothermic nature of the process is well explained by the positive value of the enthalpy change, thereby meaning that increasing

temperature will favor the adsorption of metal ions onto the pomegranate peel activated carbon. The negative value of ΔG° shows a spontaneous process at 293 K. As the temperature increases, the value of ΔG° decreases. The positive value of ΔS° is corroborated by the increased randomness and disorder at the solid/solution interface during the adsorption of copper ions onto PPAC. Besides, the positive ΔS° value indicates that the biosorption process is entropy-governed rather than the enthalpy governed.³⁰

FTIR before and after copper adsorption

Figure 15 reveals the difference in the FTIR spectra of PPAC before and after copper adsorption. It can be seen that there are some modifications in the IR spectra, depicted by changes in the vibration peaks at 2340 cm⁻¹, 2990 cm⁻¹ and 3690 cm⁻¹ due to chemical changes.³³ The band at 989 cm⁻¹, characteristic of P-containing groups, plays an important role in the Cu (II) adsorption, which is consistent with the research results of Gao *et al.*⁵⁴

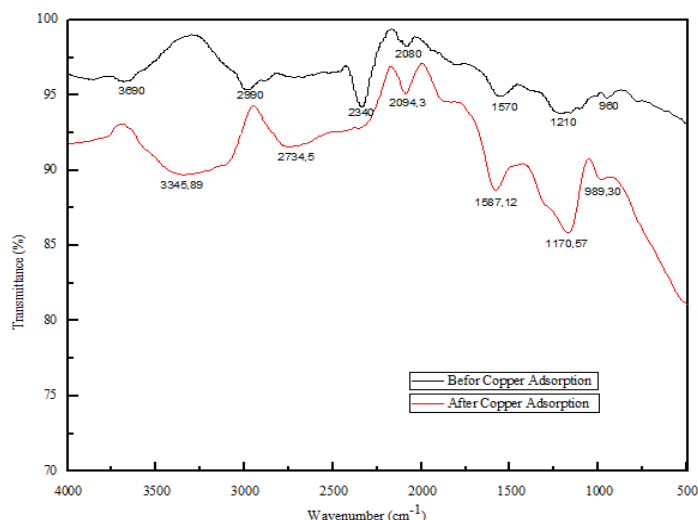


Figure 15: FTIR spectra of PPAC before and after copper adsorption

REFERENCES

- ¹ D. Mohan, C. U. Pittman and P. H. Steele Single, *J. Colloid Interface Sci.*, **297**, 489 (2006), <http://doi.org/10.1016/j.jcis.2005.11.023>
- ² D. Mohan and K. P. Singh, *Water Res.*, **36**, 2304 (2002), [http://doi.org/10.1016/s0043-1354\(01\)00447-x](http://doi.org/10.1016/s0043-1354(01)00447-x)
- ³ R. Naseem and S. S. Tahir, *Water Res.*, **33**, 3982 (2011), [http://doi.org/10.1016/s0043-1354\(01\)00130-0](http://doi.org/10.1016/s0043-1354(01)00130-0)
- ⁴ R. Boussahel, PhD Thesis, Université de Limoges, 2001, n°17
- ⁵ T. Bohli, A. Ouederni, N. Fiol and I. Villaescusa, *C. R. Chim.*, **18**, 88 (2015), <http://doi.org/10.1016/j.crci.2014.05.009>
- ⁶ J. Song, R. Zhang, K. Li, B. Li and C. Tang, *Clean – Soil Air Water*, **43**, 79 (2015), <http://doi.org/10.1002/clen.201300533>
- ⁷ H. Demiral and C. Güngör, *J. Clean. Prod.*, **124**, 103 (2016), <http://doi.org/10.1016/j.jclepro.2016.02.084>
- ⁸ E. Vunain, D. Kenneth and T. Biswick, *Appl. Water Sci.*, **7**, 430 (2017), <http://doi.org/10.1007/s13201-017-0573-x>
- ⁹ M. M. Rao, A. Ramesh, G. P. C. Rao and K. Seshaiyah, *J. Hazard. Mater.*, **129**, 123 (2006), <http://doi.org/10.1016/j.jhazmat.2005.08.018>
- ¹⁰ M. Kobya, E. Demirbas, E. Senturk and M. Ince, *Biorecour. Technol.*, **96**, 1518 (2005), <http://doi.org/10.1016/j.biortech.2004.12.005>
- ¹¹ M. H. Kalavathy, T. Karthikeyan, S. Rajgopal and L. R. Miranda, *J. Colloid Interface Sci.*, **292**, 354 (2005), <http://doi.org/10.1016/j.jcis.2005.05.087>
- ¹² K. Wilson, H. Yang and W. E. Marshall, *Bioresour. Technol.*, **97**, 2266 (2006), <http://doi.org/10.1016/j.biortech.2005.10.043>
- ¹³ X. Gao, L. Wu, Q. Xu, W. Tian, Z. Li *et al.*, *Environ. Sci. Pollut. Res.*, **25**, 7907 (2018), <http://doi.org/10.1007/s11356-017-1079-7>
- ¹⁴ E. S. Z. El-Ashtoukhy, N. K. Amin and O. Abdelwahab, *Desalination*, **223**, 162 (2008), <https://doi.org/10.1016/j.desal.2007.01.206>
- ¹⁵ S. Ben Ali, *Int. J. Chem. Eng.*, **2021**, 1 (2021), <https://doi.org/10.1155/2021/8840907>
- ¹⁶ W. A. Al-Onazi, M. H. H. Ali and T. Al-Garni, *J. Chem.*, **2021**, 1 (2021), <https://doi.org/10.1155/2021/5514118>
- ¹⁷ Y. Boutaleb, R. Zerdoum, N. Bensid, R. A. Abumousa, Z. Hattab *et al.*, *Water*, **14**, 1 (2022), <https://doi.org/10.3390/w14233885>
- ¹⁸ Y. A. B. Neolaka, A. A. P. Riwu, U. O. Aigbe, K. E. Ukhurebor, R. B. Onyancha *et al.*, *Results in Chemistry*, **5**, 1 (2023), <https://doi.org/10.1016/j.rechem.2022.100711>
- ¹⁹ W. Saadi, S. Najar-Souissi and A. Ouederni, *J. Int. Environ. Appl. Sci.*, **11**, 118 (2016), <https://dergipark.org.tr/en/pub/jieas/issue/40291/480816>
- ²⁰ M. E. Elhussien, M. A. Abdelraheem, R. M. Hussein and M. H. Elsaïm, *Adv. Biochem.*, **5**, 89 (2017), <http://doi.org/10.11648/j.ab.20170505.12>
- ²¹ J. Serafin, U. Narkiewicz, A. W. Morawski, R. J. Wróbel and B. Michalkiewicz, *J. CO₂ Util.*, **18**, 73 (2017), <http://doi.org/10.1016/j.jcou.2017.01.006>
- ²² S. N. Souissi, W. Saadi, M. Zarroug and A. Ouederni, *J. Eng. Appl. Sci.*, **14**, 6731 (2019), <https://doi.org/10.36478/jeasci.2019.6731.6741>
- ²³ W. Saadi, S. Rodríguez-Sánchez, B. Ruiz, S. Najar-Souissi, A. Ouederni *et al.*, *J. Environ. Chem. Eng.*, **10**, 107010 (2022), <http://doi.org/10.1016/j.jece.2021.107010>
- ²⁴ M. Zarroug, S. Najar-Souissi and A. Ouederni, *Fifth International Renewable Energy Congress IREC'2014*, IEEE, 2014
- ²⁵ I. Langmuir, *J. Am. Chem. Soc.*, **40**, 1361 (1918), <http://doi.org/10.1021/ja02242a004>
- ²⁶ H. M. F. Freundlich, *Z. Phys. Chem.*, **57**, 385 (1906)
- ²⁷ M. I. Temkin and V. Pyzhev, *Acta Physico Chim. U.S.S.R.*, **12**, 327 (1940)
- ²⁸ S. Lagergren, *K. Sven. Vetenskapsakad. Handl.*, **24**, 1 (1898)
- ²⁹ Y. S. Ho and G. McKay, *Water Resour.*, **34**, 735 (2000), [http://doi.org/10.1016/s0043-1354\(99\)00232-8](http://doi.org/10.1016/s0043-1354(99)00232-8)
- ³⁰ H. N. Tran, S. J. You and H. P. Chao, *J. Environ. Chem. Eng.*, **4**, 2671 (2016), <http://doi.org/10.1016/j.jece.2016.05.009>
- ³¹ K. S. K. Reddy, A. Al Shoaibi and C. Srinivasakannan, *New Carbon Mater.*, **27**, 344 (2012), [http://doi.org/10.1016/s1872-5805\(12\)60020-1](http://doi.org/10.1016/s1872-5805(12)60020-1)
- ³² A. Gundogdu, C. Duran, H. B. Senturk, M. Soylak, M. Imamoglu *et al.*, *J. Anal. Appl. Pyrol.*, **104**, 249 (2013), <http://doi.org/10.1016/j.jaap.2013.07.008>
- ³³ M. I. Sabela, K. Kunene, S. Kanchi, M. X. Nokukhanya, A. Bathinapatla *et al.*, *Arab. J. Chem.*, **12**, 4331 (2019), <http://doi.org/10.1016/j.arabjc.2016.06.001>
- ³⁴ T. Senthilkumar, R. Raghuraman and L. R. Miranda, *Clean – Soil Air Water*, **41**, 797 (2013), <http://doi.org/10.1002/clen.201100719>
- ³⁵ S. M. Yakout and G. Sharaf El-Deen, *Arab. J. Chem.*, **9**, S1155 (2016), <http://doi.org/10.1016/j.arabjc.2011.12.002>
- ³⁶ IUPAC (International Union of Pure and Applied Chemistry), *Pure Appl. Chem.*, **57**, 603 (1985), <http://dx.doi.org/10.1351/pac198557040603>
- ³⁷ K. Bellir, M. B. Lehocine and A. H. Meniai, *Desalin. Water Treat.*, **51**, 5035 (2013), <http://doi.org/10.1080/19443994.2013.808786>
- ³⁸ Y. P. Teoh, M. A. Khan and T. S. Y. Choong, *Chem. Eng. J.*, **217**, 248 (2013), <http://doi.org/10.1016/j.cej.2012.12.013>
- ³⁹ M. A. P. Cechinel, S. M. de Souza and A. A. U. de Souza, *J. Clean. Prod.*, **65**, 342 (2014), <http://doi.org/10.1016/j.jclepro.2013.08.020>

- ⁴⁰ M. E. Argun, S. Dursun, C. Ozdemir and M. Karatas, *J. Hazard. Mater.*, **141**, 77 (2007), <http://doi.org/10.1016/j.jhazmat.2006.06.095>
- ⁴¹ A. Roy and J. Bhattacharya, *Sep. Purif. Technol.*, **115**, 172 (2013), <http://doi.org/10.1016/j.seppur.2013.05.010>
- ⁴² M. Momcilovic, M. Purenovic, A. Bojic, A. Zarubica and M. Randelovic, *Desalination*, **276**, 53 (2011), <http://doi.org/10.1016/j.desal.2011.03.013>
- ⁴³ T. Depci, A. R. Kul and Y. Onal, *Chem. Eng. J.*, **200-202**, 224 (2012), <http://doi.org/10.1016/j.cej.2012.06.077>
- ⁴⁴ J. Shou and M. Qiu, *Desalin. Water Treat.*, **57**, 353 (2014), <http://doi.org/10.1080/19443994.2014.966328>
- ⁴⁵ C. H. Weng, C. Z. Tsai, S. H. Chu and Y. C. Sharma, *Sep. Purif. Technol.*, **54**, 187 (2007), <http://doi.org/10.1016/j.seppur.2006.09.009>
- ⁴⁶ A. H. Sulaymon, B. A. Abid and J. A. Al-Najar, *Chem. Eng. J.*, **155**, 647 (2009), <http://doi.org/10.1016/j.cej.2009.08.021>
- ⁴⁷ K. G. Sreejalekshmi, K. K. Anoop and T. S. Anirudhan, *J. Hazard. Mater.*, **161**, 1506 (2009), <http://doi.org/10.1016/j.jhazmat.2008.05.002>
- ⁴⁸ R. A. K. Rao and F. Rehman, *Adsorpt. Sci. Technol.*, **28**, 195 (2010), <https://doi.org/10.1260/0263-6174.28.3.195>
- ⁴⁹ S. Ben Ali, I. Jaouali, S. Souissi-Najar and A. Ouederni, *J. Clean. Prod.*, **142**, 3809 (2017), <http://doi.org/10.1016/j.jclepro.2016.10.081>
- ⁵⁰ F. Sakr, A. Sennaoui, M. Elouardi, M. Tamimi and A. Assabbane, *J. Mater. Environ. Sci.*, **6**, 397 (2015)
- ⁵¹ D. Hu and L. Wang, *J. Taiwan Inst. Chem. Eng.*, **64**, 227 (2016), <http://doi.org/10.1016/j.jtice.2016.04.028>
- ⁵² M. H. Kalavathy, T. Karthikeyan, S. Rajgopal and L. R. Miranda, *J. Colloid Interf. Sci.*, **292**, 354 (2005), <https://doi.org/10.1016/j.jcis.2005.05.087>
- ⁵³ Y. S. Ho and G. McKay, *Process Biochem.*, **34**, 451 (1999), [http://doi.org/10.1016/S0032-9592\(98\)00112-5](http://doi.org/10.1016/S0032-9592(98)00112-5)
- ⁵⁴ X. Gao, L. Wu, Q. Xu, W. Tian, Z. Li et al., *Environ. Sci. Pollut. Res.*, **25**, 7907 (2018), <http://doi.org/10.1007/s11356-017-1079-7>
- ⁵⁵ V. Kulkarni, A. Golder and P. Ghosh, *J. Water Process. Eng.*, **18**, 92 (2017), <https://doi.org/10.1016/j.jwpe.2017.06.009>
- ⁵⁶ S. Taha, S. Ricordel and I. Cisse, *Energ. Proc.*, **6**, 143 (2011), <http://doi.org/10.1016/j.egypro.2011.05.017>
- ⁵⁷ L. Renugopal, K. W. Kow, P. L. Kiew, S. P. Yeap, H. S. Chua et al., in *Procs. 6th International Conference on Environment (ICENV2018), AIP Conf. Proc. 2124, 020001-1–020001-8*, 2019, <https://doi.org/10.1063/1.5117061>